Universal nonlinear conductivity close to an itinerant-electron quantum critical point

P. M. Hogan and A. G. Green
School of Physics and Astronomy, University of St. Andrews, North Haugh, St. Andrews KY16 9SS, United Kingdom
(Received 18 May 2008; revised manuscript received 20 August 2008; published 7 November 2008)

We study the conductivity in itinerant-electron systems near to a magnetic quantum critical point. We show that, for a class of geometries, the universal power-law dependence of resistivity upon temperature may be reflected in a universal nonlinear conductivity; when a strong electric field is applied, the resulting current has a universal power-law dependence upon the applied electric field. For a system with thermal-equilibrium current proportional to T^{α} and dynamical exponent z, we find a nonlinear resistivity proportional to $E^{(z-1)/[z(1+\alpha)-1]}$.

DOI: 10.1103/PhysRevB.78.195104 PACS number(s): 75.40.−s, 72.10.Di, 72.90.+y, 75.30.Kz

The notion of quantum criticality provides one of the few unifying theoretical principles of strongly correlated electrons.[1–3] It describes a range of phenomena in systems that are near to continuous zero-temperature phase transitions: phase transitions that are driven by quantum rather than thermal fluctuations. In thermal equilibrium, quantum critical systems show characteristic spatial and temporal scaling in their response to external probes. For example, the conductivity of an itinerant-electron system near to a magnetic quantum phase transition has a power-law dependence upon temperature.[4–6]

The behavior of quantum critical systems out of thermal equilibrium has begun to attract growing attention over the past few years. Near to a quantum phase transition all of the intrinsic energy scales of a system, other than the Fermi energy, renormalize to zero. In thermal equilibrium, the only remaining energy scale is the temperature itself. Because of this, quantum critical systems are particularly susceptible to being driven out of equilibrium by external probes. In certain situations the universal temporal scaling near to the quantum critical point may reveal itself in universal features of the steady-state adopted out of equilibrium: the out-of-equilibrium state being largely determined by a system's dynamics.

Several recent works have addressed the question of whether universality persists when a quantum critical system is driven out of thermal equilibrium by the application of a strong electric field. In particular, Dalidovich and Phillips, [7] and Green *et al.*[8,9] considered two-dimensional superconductor-insulator transitions,[10,11] the former in the case where the quantum dynamics and phase transition were controlled by coupling to a Caldeira-Leggett bath and the latter in the case of intrinsic superconducting dynamics. These systems can indeed display universality out of equilibrium[12] in both their current response[7,8] and their current noise statistics.[9] The triumph of Dalidovich and Phillips,[7] and Green and Sondhi[8] was to provide field-theoretical derivations of the scaling predicted by naive dimensional analysis. Numerical studies of related one-dimensional systems produced similar results.[13]

While these works provide interesting proofs of principle—and indeed, may yet be compared with experiment—most quantum critical systems that are studied experimentally are of a rather different type. The critical modes at the superconductor-insulator transition are charged and couple directly to the electric field. A more typical situation has critical modes without a charge—often magnetic—which affect transport by scattering from electrons. Here we address the question of whether universal nonlinear response in transport occurs in this more general setting.

We find that given certain conditions on size and geometry, quantum critical itinerant magnets show a universal nonlinear current response. For a long narrow sample, with an electric field applied along its length, we predict a universal nonlinear scaling of current with field given by

$$j \propto E^{(z-1)/[z(1+\alpha)-1]}, \qquad (1)$$

where the thermal-equilibrium resistivity is proportional to T^{α} and z is the dynamical exponent. In the case of the Moriya-Hertz-Millis model[4–6] of the critical ferromagnet, $\alpha=(d+z-1)/z$. Provided that certain constraints upon the dimension of the system are satisfied, this result does not depend further upon the system dimensions. In the following, we will take some time to discuss this matter and compare our results to those of related works.

We hope that these results will provide an alternative experimental window upon quantum criticality. Despite its successes, the theory of itinerant-electron quantum criticality has some puzzling problems; although power-law dependencies upon temperature are seen experimentally, there is often a discrepancy between the observed and predicted powers in transport. Nonlinear response may help to resolve this issue by providing two consistency checks: whether the equilibrium exponents are consistent with the out-of-equilibrium exponents through Eq. (1) and whether the out-of-equilibrium exponent is consistent with the Moriya-Hertz-Millis theory.[4–6]

Our paper is outlined as follows. We begin in Sec. I with a general description of our scheme, paying particular attention to matters of geometry and heat flows within the system. This will enable a heuristic derivation of our main results and a detailed comparison with the complementary work of Mitra *et al.*[14] In Sec. II, we will begin with a survey of the Boltzmann treatment of the linear response of the itinerant-electron quantum critical system in thermal equilibrium. This will allow us to introduce some notation and familiarize the reader with its application in this context. We follow this in Sec. III by applying the Boltzmann transport formalism to the out-of-equilibrium system. This section contains a formal derivation of our main results. Finally, in Sec. IV, we turn to a discussion of the limitations of our analysis and of the prospects for seeing the effects that we predict in experiment.

I. GENERAL SCHEME

Geometry. We consider a long narrow quantum critical itinerant-electron system with an electric field applied along its length. The system is longer than its transport length so that an electron traversing the sample scatters from paramagnons many times. The system must also be wide enough that it displays bulk behavior, but narrow enough that heat generated within the sample can be transported to the boundary.

Critical fields. Starting from some low base temperature, T_0, and gradually increasing the electric field one may anticipate two fields at which the response may become nonlinear.

(i) When the energy gained by an electron from the electric field between scattering events exceeds the temperature,

$$E_1 \sim \frac{T_0}{l_{\mathrm{tr}}},$$

where l_{tr} is the transport scattering length.

(ii) When the Joule heating rate exceeds the rate at which heat may be transported from the sample by a transverse heat flow,

$$E_2^2\sigma \sim \kappa T_0/W^2 \Rightarrow E_2 \sim \frac{T_0}{W}\sqrt{l_{\mathrm{th}}/l_{\mathrm{tr}}},$$

where σ and κ are the electrical and thermal conductivities. The latter result has been obtained using $\kappa/\sigma T_0 = l_{\mathrm{th}}/l_{\mathrm{tr}}$. l_{th} is the thermal scattering length and W is the sample width.

In this work, we will be primarily concerned with the former case. In order for a system to be in this regime, we require that $E_1 \ll E_2$, so that we hit the field E_1 first when increasing the electric field from zero; i.e., we require that $W \ll \sqrt{l_{\mathrm{tr}} l_{\mathrm{th}}}$. In addition, for the system to exhibit bulk behavior requires that it be wider than its correlation length, $W \gg l_{\mathrm{th}}$. Combining these two conditions upon the sample width yields

$$l_{\mathrm{th}} \ll W \ll \sqrt{l_{\mathrm{tr}} l_{\mathrm{th}}}. \tag{2}$$

Due to additional angular factors, the transport length is substantially greater than the thermal scattering length, $l_{\mathrm{tr}} \gg l_{\mathrm{th}}$, so that there is a large window of sample widths over which the type of nonlinear response that we envisage can occur. In the high-temperature limit (with $T \ll \epsilon_F$ nevertheless) in which experimental investigations of itinerant-electron quantum criticality are usually carried out, $l_{\mathrm{tr}} \sim l_{\mathrm{th}}/\theta^2$, where $\theta \sim q/k_F \sim (T/\epsilon_F)^{1/z}$ is the angle of scattering.

This regime is somewhat delicately balanced between the macroscopic and microscopic. In a truly macroscopic sample where $W \to \infty$, nonlinearity always occurs due to the failure to conduct away excess Joule heat. In our case, the transverse size of the system must be small enough that $W \ll \sqrt{l_{\mathrm{tr}} l_{\mathrm{th}}}$, but the system inherits its behavior from macroscopic equilibrium properties since it is larger than the correlation length.[15] If the above constraints are satisfied, the nonlinear transport properties depend only upon bulk properties and are independent of the dimensions of the system.

Thermal coupling. Determining the nonlinear response requires keeping careful track of the various heat flows. We consider a simplified scheme of thermal couplings in our sample.

(i) The electrons couple to a heat sink at the boundaries of the sample and scatter from paramagnons. We do not consider electron-electron scattering since this is higher order in temperature or electric field than electron-paramagnon scattering and so subleading at low temperatures and fields.

(ii) The paramagnons may scatter both from one another and from the electrons. We do not consider coupling between paramagnons and the heat sink. Our reason is that paramagnon-phonon relaxation is higher order in temperature or field than paramagnon-electron scattering and therefore weaker at low temperatures and field.

Heuristic treatment. Given these descriptions of the geometry of our system and the various microscopic couplings, we are now in a position to give a heuristic derivation of our main results. Heat enters the system via Joule heating and ultimately leaves through a transverse heat flow maintained by a transverse variation in temperature. In the absence of direct scattering between electrons, this energy must pass through the paramagnon subsystem: Joule heating pumps energy into higher moments of the electron distribution. This is ultimately carried away by a transverse heat flow maintained by a gradient in the symmetrical part of the electron distribution. Energy can only pass into the symmetrical part of the distribution due to scattering via paramagnons. In leading approximation, the paramagnon subsystem is raised to an effective temperature $T_{\mathrm{eff}}(E)$ determined by a balance between the Joule heating rate and the rate at which the paramagnon subsystem at $T_{\mathrm{eff}}(E)$ loses energy to the electron subsystem at $T_0 \sim 0$. Equating these two rates of change in energy leads to a self-consistency equation for T_{eff}.

In the high-temperature limit, the scattering time τ, the transport scattering time τ_{tr}, and the paramagnon energy decay rate $d\xi/dt$ are related as follows:

$$\frac{1}{\tau_{\mathrm{tr}}} \sim \frac{T^{2/z}}{\tau},$$

$$\frac{d\mathcal{E}}{dt} \sim \frac{T^2}{\tau}.$$

Using these relations for a system whose thermal-equilibrium resistivity scales as T^α, we find

$$\text{Joule heating} \propto \sigma E^2 \propto E^2 T_{\mathrm{eff}}^{-\alpha},$$

$$\text{Energy relaxation} \propto T_{\mathrm{eff}}^{2(1-1/z+\alpha)},$$

$$\frac{d\mathcal{E}}{dt} = \sigma E^2. \tag{3}$$

By equating these two rates we deduce that $T_{\mathrm{eff}} \propto E^{z/[z(1+\alpha)-1]}$ and $j \propto E^{(z-1)/[z(1+\alpha)-1]}$. In Secs. I and II we will flesh out these ideas with particular reference to the Moriya-Hertz-Millis model[4–6] of the critical ferromagnet.

Comparison with Mitra et al.[14] A recent work of Mitra *et al.*[14] has considered the same system as studied here but in a different geometry. The results obtained in Ref. 14 are different from ours because of this geometry. In order to allay any confusion, it is worth spending a moment to note the main distinction between our two works. Mitra *et al.*[14] considered an itinerant-electron system with essentially two-dimensional geometry and an electric field applied in the third short direction. In this case, an electron traversing the sample from one lead to another does not scatter appreciably from paramagnons—the electron distribution is determined to leading order by the distributions in the leads and may be written directly in terms of them using a Keldysh formalism. Mitra *et al.*[14] presented an appealing derivation of this zeroth-order distribution and showed, using a renormalization-group analysis, that an effective temperature proportional to the applied voltage results. In our case, by contrast, an electron traversing the sample between the two leads scatters many times off paramagnons and the electron distribution must be calculated self-consistently from the start.[16]

In the rest of this paper, we will spend some time fleshing out the mathematical details of this general scheme. We begin in Sec. II by reviewing the Boltzmann approach to thermal-equilibrium transport in quantum critical metals.

II. BOLTZMANN APPROACH IN THERMAL EQUILIBRIUM

We will use Boltzmann transport techniques to analyze the out-of-equilibrium response of a quantum critical system to an electric field. Although this approach is familiar in other contexts, itinerant-electron quantum critical transport is usually analyzed by other means. Therefore, in this section, we will spend a little time summarizing quantum critical transport in thermal equilibrium and how this may be described using a Boltzmann equation approach. This exposition will also serve as a useful way of defining the notation that we will use later in our analysis of the nonlinear response.

Our first step will be to describe the thermal-equilibrium paramagnon propagator. We follow this by writing down the electron Boltzmann equation and construct its linear-response solution. Finally, we quote a number of relaxation rates that will be useful in our nonequilibrium analysis. The details of the calculation of these within a Boltzmann framework are somewhat similar to that of the relaxation rates due to phonon scattering. We sketch these calculations in Appendix A.

A. Paramagnon propagator

We work within the Moriya-Hertz-Millis approach[4–6] to itinerant-electron quantum criticality. The bosonic magnetic critical modes—the paramagnons—are treated separately from the electrons (although they are, of course, made from electrons so that care must be taken to avoid double counting of degrees of freedom[17]). The effects of scattering between the paramagnons and electrons are treated self-consistently: the paramagnon dynamics being determined by Landau damping and the electronic transport being determined by scattering from the paramagnon fluctuations.

The first step in the Moriya-Hertz-Millis approach[4–6] to itinerant-electron quantum criticality is to determine the critical properties of the paramagnons. These critical properties are the combined result of the paramagnons' self-interaction and their overdamped dynamics due to Landau damping. The simplest way to do this is through the self-consistent renormalization group.[4] Alternatively, one may use a more rigorous application of the renormalization group[5,6] in order to obtain essentially the same results. In either case, the critical paramagnon propagator takes on the following form in the equilibrium quantum critical state:

$$D^R(\boldsymbol{q},\omega) = \left[i\frac{|\omega|}{\Gamma_{\boldsymbol{q}}} + \boldsymbol{q}^2 + r(T) \right]^{-1}, \tag{4}$$

where $\Gamma_{\boldsymbol{q}}$ describes the Landau damping. $\Gamma_{\boldsymbol{q}}$ is proportional to $|\boldsymbol{q}|$ in the ferromagnet and constant in an antiferromagnet (or $\Gamma_{\boldsymbol{q}}=\Gamma|\boldsymbol{q}|^{z-2}$ in general). The paramagnon gap $r(T)$ takes on characteristic power-law forms in temperature in the quantum critical system,

$$r(T) \propto T^{(d+z-2)/z}, \tag{5}$$

where d is the dimension and z is the dynamical exponent ($z=3$ in the ferromagnet and 2 in the antiferromagnet). Through most of our subsequent analysis, we shall concentrate upon the situation in three dimensions. This is readily extended to other dimensions. The overdamping of paramagnons has important consequences. Unlike their phonon counterparts, paramagnon excitations do not have a well-defined energy for a particular wave vector. This does not have enormous consequences for a Boltzmann analysis in thermal equilibrium, but it does necessitate modification of the paramagnon Boltzmann equation when we consider the out-of-equilibrium situation.

A peculiarity of our analysis is that since we are interested in electrical transport, we will describe the system mainly in terms of the electronic degrees of freedom rather than the critical paramagnons. The key length scales to which we refer—such as the thermal and transport scattering lengths—are length scales for the electron dynamics and not for the critical paramagnons. The underlying critical paramagnons have only one important length scale—the correlation length $r(T)^{-1/2}$—as is usual in a critical system. The electronic length scales are somewhat longer than this because of the small energy/momentum transfer in electron-paramagnon scattering events.

B. Boltzmann equation

The electronic Boltzmann equation for scattering from an uncharged auxiliary mode may be written as

$$[\partial_t + (e\boldsymbol{E}/\hbar)\cdot\partial_{\boldsymbol{k}}]f_{\boldsymbol{k}} = -\int \frac{d\mathbf{q}}{(2\pi)^3}[\gamma_{\boldsymbol{kq}}f_{\boldsymbol{k}}(1-f_{\boldsymbol{q}}) - \gamma_{\boldsymbol{qk}}f_{\boldsymbol{q}}(1-f_{\boldsymbol{k}})]. \tag{6}$$

The matrices $\gamma_{\boldsymbol{kq}}$ describe scattering from the auxiliary modes—paramagnons in our case. Quite generally, for scattering from auxiliary modes that have a thermal distribution, the scattering matrices satisfy the detailed balance relationship,

$$\gamma_{kq} = \gamma_{qk} \exp[(\epsilon_k - \epsilon_q)/T]. \tag{7}$$

In the case of paramagnon scattering, the scattering matrices take the form

$$\begin{aligned}\gamma_{pq} = |g_{q-p}|^2\{[1 + n(\epsilon_p - \epsilon_q)]\rho(\boldsymbol{p} - \boldsymbol{q}, \epsilon_p - \epsilon_q) \\ + n(\epsilon_q - \epsilon_p)\rho(\boldsymbol{q} - \boldsymbol{p}, \epsilon_q - \epsilon_p)\},\end{aligned} \tag{8}$$

where g_{q-p} is the matrix element for electron-paramagnon scattering and $\rho(\boldsymbol{q}, \omega)$ is the paramagnon spectral function. In antiferromagnets, the matrix element g_{q-p} has significant momentum dependence, with scattering hot spots corresponding to resonance of the magnetic ordering wave vector with the Fermi surface. For simplicity, we restrict our analysis to the case of ferromagnets or long-wavelength helimagnets where the momentum dependence of g_{q-p} is weak and can be neglected. The paramagnon spectral function is given by

$$\rho(\boldsymbol{q}, \omega) = -\frac{1}{\pi}\mathcal{I}mD^R(\boldsymbol{q}, \omega) = \frac{\omega/\Gamma_q}{(r + \boldsymbol{q}^2)^2 + (\omega/\Gamma_q)^2}. \tag{9}$$

It is determined by the paramagnon propagator given in Eq. (4). It contains all of the information about how dynamics is incorporated into the critical behavior through the relative scaling of frequency and momentum: $\omega \sim q^z \sim q^2\Gamma_q$. In what follows, it will prove very useful to work with the general form of the Boltzmann equation [Eq. (6)] rather than the form obtained after explicit substitution of γ_{pq}.

C. Linear response solution of the Boltzmann equation

The generic notation of Eq. (6) allows us to construct a formal linear-response solution of the Boltzmann equation both in thermal equilibrium and, ultimately, out of thermal equilibrium. In order to orient ourselves for the latter more involved calculation, let us first construct the conventional linear-response solution with this general notation. Identifying[9]

$$\mathbf{M}_{kq} = \frac{\gamma_{qk}}{\gamma_k}\frac{1 - f_k}{1 - f_q} \qquad \gamma_k = \int d\boldsymbol{q}\, \gamma_{kq}\frac{1 - f_q}{1 - f_k} \tag{10}$$

and adopting an Einstein convention with implied integration over the momentum $\boldsymbol{q}$, but not $\boldsymbol{k}$, we may write the Boltzmann equation in the form

$$[\partial_t + (e\boldsymbol{E}/\hbar) \cdot \partial_k]f_k = -\gamma_k[1 - \mathbf{M}]_{kq}f_q(1 - f_q). \tag{11}$$

Let us consider an initial thermal distribution of electrons and auxiliary modes at the same temperature. The deviation in the electron distribution from its initial thermal distribution, f_k^0, in response to an electric field is given by a solution of the linearized equation,

$$(e\boldsymbol{E}/\hbar) \cdot \partial_k[f_k^0 + \delta f_k] = -\gamma_k[1 - \mathbf{M}]_{kq}\delta f_q, \tag{12}$$

where an Einstein convention has again been adopted. There are a couple of steps required in deriving this equation. First, we have used the fact that the scattering integral is zero when the electrons and paramagnons are in thermal distributions at the same temperature. One must also allow for the dependence of $[1-\mathbf{M}]_{kq}$ upon f_q in obtaining the first functional derivative of the scattering integral.

A formal solution to the linearized Boltzmann equation [Eq. (12)] is readily obtained. Expanding to linear order in the electrical field we find

$$\delta f_k = [1 - \mathbf{M}]^{-1}_{kq}\frac{1}{\gamma_q}\boldsymbol{E} \cdot \partial_q f_q. \tag{13}$$

This result may be integrated to obtain the current that flows in response to the application of the electric field,

$$\boldsymbol{j} = \int \frac{d\boldsymbol{k}}{(2\pi)^d}\boldsymbol{k}\,\delta f_k = \int \frac{d\boldsymbol{k}}{(2\pi)^3}\frac{d\boldsymbol{q}}{(2\pi)^3}\boldsymbol{k}[1 - \mathbf{M}]^{-1}_{kq}\frac{1}{\gamma_q}\boldsymbol{E} \cdot \partial_q f_q, \tag{14}$$

where an explicit integral over $\boldsymbol{k}$ has been restored. In Sec. III, we will turn to a consideration of the nonlinear response of the electron-paramagnon system using a very similar Boltzmann transport analysis. Before this, we identify a number of different time scales of relevance to our problem and calculate them in the case of paramagnon scattering.

D. Compendium of relaxation rates

The electronic scattering integral is given by the right-hand side of Eq. (6) and (12),

$$\begin{aligned}\left(\frac{\partial f_q}{\partial t}\right)_{\text{scatt}} &= -\int \frac{d\boldsymbol{p}}{(2\pi)^3}[\gamma_{qp}f_q(1 - f_p) - \gamma_{pq}f_p(1 - f_q)] \\ &= -\gamma_q[1 - \mathbf{M}]_{qp}f_p(1 - f_p) = -\gamma_q[1 - \mathbf{M}]_{qp}\delta f_p,\end{aligned} \tag{15}$$

where γ_q and $\mathbf{M}_{qp}$ are given by Eq. (10). Integration over $\boldsymbol{p}$ has been suppressed in the final two expressions, which are drawn from Eqs. (11) and (12), respectively.

We may identify several different time scales from this scattering integral that will appear in our later study of the nonequilibrium response,

$$\frac{1}{\tau_q} = \gamma_q = \int \frac{d\boldsymbol{p}}{(2\pi)^3}\gamma_{qp}\frac{1 - f_p}{1 - f_q},$$

$$\frac{1}{\tau_q^{\text{tr}}} = \gamma_q^{\text{tr}} = \int \frac{d\boldsymbol{p}}{(2\pi)^3}\gamma_{qp}\frac{1 - f_p}{1 - f_q}\left[1 - \frac{\boldsymbol{q} \cdot \boldsymbol{p}}{q^2}\frac{\gamma_q^{\text{tr}}}{\gamma_p^{\text{tr}}}\right],$$

$$\frac{d\mathcal{E}}{dt} = \frac{1}{2}\int \frac{d\boldsymbol{p}}{(2\pi)^3}\frac{d\boldsymbol{q}}{(2\pi)^3}(\epsilon_q - \epsilon_p)[\gamma_{qp}f_q^0(1 - f_p^0) - \gamma_{pq}f_p^0(1 - f_q^0)]. \tag{16}$$

The first of these scattering rates is simply the inverse time between collisions. The second is the transport scattering rate. This has the usual additional geometrical factor arising since large-angle scattering has more effect upon transport than small-angle scattering.[18] The ratio $\gamma_q^{\text{tr}}/\gamma_p^{\text{tr}}$ is conventionally set to 1 since we are interested in the scattering of fermions near to the Fermi surface. The final expression is the rate of flow of energy from the auxiliary-mode subsystem at a temperature T (at which γ_{pq} is evaluated) to the electron subsystem at temperature T_0 (indicated by the superscript 0 on the electron distribution functions).

In the high-temperature limit, these relaxation rates have the following temperature dependence within the Moriya-Hertz-Millis theory[4–6] in d dimensions:

$$1/\tau \propto T^{(d+z-3)/z},$$

$$1/\tau_{\mathrm{tr}} \propto T^{(d+z-1)/z},$$

$$d\mathcal{E}/dt \propto T^{(d+3z-3)/z}. \tag{17}$$

Details of how to get these results from Eqs. (16) are given in Appendix A. After these preliminaries, we are now in a position to adapt our Boltzmann equation to describe the out-of-equilibrium behavior of our system.

III. NONEQUILIBRIUM RESPONSE

In this section we will turn the machinery of Boltzmann transport to the question of nonequilibrium behavior in the itinerant critical ferromagnet. As discussed earlier, for a system to have an out-of-equilibrium steady state under the application of an electric field, it must be coupled to a heat sink that can dissipate the excess energy generated by Joule heating. We must pay careful attention to the various thermal couplings. The nature of these bears repetition at this juncture.

As described in Sec. I, we consider a long narrow sample in which the excess Joule heat is carried away by a transverse heat current to a heat sink at the edge. Heat entering the electron subsystem via Joule heating passes to the paramagnon subsystem and then back to the electron subsystem via mutual scattering and leaves the electron subsystem via coupling to a heat sink at the boundary. The paramagnons themselves interact both with the electrons and with one another. Electron-electron scattering is neglected in our analysis—it is higher order in temperature and hence field—as is coupling of paramagnons directly to the heat sink.

Our analysis is divided into three parts. We begin by writing down the Boltzmann equations for the electron-paramagnon system. These equations embody the various thermal couplings and interactions in our system. The only subtlety enters through the form of the paramagnons' Boltzmann equation: the overdamped nature of the paramagnon excitations leads to a slightly more complicated equation than the comparable case of phonon scattering. In fact, the details of the paramagnon Boltzmann equation will not have a huge effect upon our main result. Next, we will present formal solutions for the electron and paramagnon distribution functions. Our main results follow from consideration of these solutions in the limit where paramagnon-paramagnon scattering leads to a thermal distribution of paramagnons with temperature determined by the electric field. We will end with an argument why correction to this thermal distribution of paramagnons does not change the scaling of our results.

A. Boltzmann equation

The electron Boltzmann equation is given by a minimal modification of the thermal-equilibrium Boltzmann equation (6),

$$\begin{aligned}[\partial_t + (e\boldsymbol{E}/\hbar)\cdot\partial_{\boldsymbol{k}} + \boldsymbol{v}_{\boldsymbol{k}}\cdot\nabla]f_{\boldsymbol{k}} &= \mathbf{I}_{\boldsymbol{k}}^{em}[f,n] + \text{scattering to heat sink}\\ &= -\int\frac{d\boldsymbol{q}}{(2\pi)^3}[\gamma_{\boldsymbol{kq}}f_{\boldsymbol{k}}(1-f_{\boldsymbol{q}}) - \gamma_{\boldsymbol{qk}}f_{\boldsymbol{q}}(1-f_{\boldsymbol{k}})] + \text{heat sink},\end{aligned} \tag{18}$$

where $\mathbf{I}_{\boldsymbol{k}}^{em}[f,n]$ indicates the scattering integral for electrons of momentum $\boldsymbol{k}$ scattering from paramagnons. The gradient term $\boldsymbol{v}_{\boldsymbol{k}}\cdot\nabla$ has been added to allow for the possibility of transverse heat flow. The electron-paramagnon scattering matrices now take a slightly modified form compared to that in thermal equilibrium (8). Since the paramagnons are overdamped and as a result do not have a definite relationship between their energy and momentum, the paramagnon distribution is a function of both energy and momentum. Taking this into account, the scattering matrices take the form

$$\begin{aligned}\gamma_{\boldsymbol{pq}} = |g_{\boldsymbol{q}-\boldsymbol{p}}|^2\{&[1+n_{\boldsymbol{p}-\boldsymbol{q}}(\epsilon_{\boldsymbol{p}}-\epsilon_{\boldsymbol{q}})]\rho(\boldsymbol{p}-\boldsymbol{q},\epsilon_{\boldsymbol{p}}-\epsilon_{\boldsymbol{q}})\\ &+ n_{\boldsymbol{q}-\boldsymbol{p}}(\epsilon_{\boldsymbol{q}}-\epsilon_{\boldsymbol{p}})\rho(\boldsymbol{q}-\boldsymbol{p},\epsilon_{\boldsymbol{q}}-\epsilon_{\boldsymbol{p}})\}.\end{aligned} \tag{19}$$

The linearized expansion about the zero-field base-temperature distribution $f_{\boldsymbol{q}}^0$ takes the form

$$\begin{aligned}(e\boldsymbol{E}/\hbar)\cdot\partial_{\boldsymbol{k}}[f_{\boldsymbol{k}}^0 + \delta f_{\boldsymbol{k}}] = -\int\frac{d\boldsymbol{q}}{(2\pi)^3}&[\gamma_{\boldsymbol{kq}}f_{\boldsymbol{k}}(1-f_{\boldsymbol{q}})\\ &- \gamma_{\boldsymbol{qk}}f_{\boldsymbol{q}}(1-f_{\boldsymbol{k}})] - \gamma_{\boldsymbol{k}}[1-\mathbf{M}]_{\boldsymbol{kq}}\delta f_{\boldsymbol{q}}\\ &+ \text{heat sink},\end{aligned} \tag{20}$$

where $\gamma_{\boldsymbol{k}}$ and $\mathbf{M}_{\boldsymbol{kq}}$ take a slightly modified form out of equilibrium given by

$$\gamma_{\boldsymbol{k}} = \int\frac{d\boldsymbol{q}}{(2\pi)^3}[\gamma_{\boldsymbol{kq}}(1-f_{\boldsymbol{q}}^0) + \gamma_{\boldsymbol{qk}}f_{\boldsymbol{q}}^0],$$

$$\gamma_{\boldsymbol{k}}\mathbf{M}_{\boldsymbol{kq}} = \gamma_{\boldsymbol{kq}}f_{\boldsymbol{k}}^0 + \gamma_{\boldsymbol{qk}}(1-f_{\boldsymbol{k}}^0). \tag{21}$$

These reduce to our previous expressions for $\gamma_{\boldsymbol{k}}$ and $\mathbf{M}_{\boldsymbol{kq}}$ in thermal equilibrium (10). The simplified forms given by Eq. (10) can be obtained by making use of the detailed balance condition, which is not satisfied out of equilibrium. A couple of points are worth making about Eq. (20). First, there is a zeroth-order term on the right-hand side. This term is not present in thermal equilibrium (it is zero upon applying the detailed balance condition). This term has a different symmetry in momentum space than the first-order term in δf and we will use this in our analysis shortly.

The added complication due to the paramagnons being overdamped is compounded when we come to write down the paramagnon Boltzmann equation in a moment. Luckily, this does not affect the bulk of our calculation. We will use the formal notation $\mathbf{I}_{\boldsymbol{k}}^{em}[f,n]$ through as much of our analysis as possible in order to keep algebra to a minimum. When we eventually substitute the particular form of the scattering integrals near to the end of the calculation, we will find that most of the integration of these scattering integrals carries over directly from the thermal-equilibrium calculation.

The paramagnon Boltzmann equation takes the form

$$\partial_t n_{\boldsymbol{k}}(\epsilon) = \mathbf{I}_{\boldsymbol{k}}^{me}[f,n] + \mathbf{I}_{\boldsymbol{k}}^{mm}[n] = \int \frac{d\boldsymbol{p}}{(2\pi)^3}\frac{d\boldsymbol{q}}{(2\pi)^3}|g_k|^2\{-n_{\boldsymbol{k}}(\epsilon)f_{\boldsymbol{p}}(1-f_{\boldsymbol{q}}) + [1+n_{\boldsymbol{k}}(\epsilon)](1-f_{\boldsymbol{p}})f_{\boldsymbol{q}}\}\delta(\epsilon+\epsilon_{\boldsymbol{p}}-\epsilon_{\boldsymbol{q}})\delta(\boldsymbol{p}-\boldsymbol{q}+\boldsymbol{k})$$
$$+\lambda\int d\epsilon_1 d\epsilon_2 d\epsilon_3 \frac{d\boldsymbol{p}_1}{(2\pi)^3}\frac{d\boldsymbol{p}_2}{(2\pi)^3}\frac{d\boldsymbol{p}_3}{(2\pi)^3}\rho(\epsilon_1,\boldsymbol{p}_1)\rho(\epsilon_2,\boldsymbol{p}_2)\rho(\epsilon_3,\boldsymbol{p}_3)\{-n_{\boldsymbol{k}}(\epsilon)n_{\boldsymbol{p}_1}(\epsilon_1)[1+n_{\boldsymbol{p}_2}(\epsilon_2)][1+n_{\boldsymbol{p}_3}(\epsilon_3)]$$
$$+[1+n_{\boldsymbol{k}}(\epsilon)][1+n_{\boldsymbol{p}_1}(\epsilon_1)]n_{\boldsymbol{p}_2}(\epsilon_2)n_{\boldsymbol{p}_3}(\epsilon_3)\}\delta(\boldsymbol{k}+\boldsymbol{p}_1-\boldsymbol{p}_2-\boldsymbol{p}_3)\delta(\epsilon+\epsilon_1-\epsilon_2-\epsilon_3). \tag{22}$$

The easiest way to see the origins of the various terms in this equation is to momentarily treat the paramagnons as if they had a definite relationship between energy and momentum. In this case, the paramagnon spectral function becomes a delta function and the scattering integrals reduce to the same form as those for electron-phonon scattering. As for the electron Boltzmann equation, we will carry out as much of our analysis as possible using the formal expressions $\mathbf{I}_{\boldsymbol{k}}^{me}[f,n]$ and $\mathbf{I}_{\boldsymbol{k}}^{mm}[n]$ for the paramagnon-electron and paramagnon-paramagnon scattering integrals.

B. Solving the Boltzmann equations

Our analysis of the Boltzmann equations [Eqs. (18) and (22)] derived above proceeds as follows: We begin by dividing the electron distribution function into two parts—a spherically symmetric part and a nonsymmetric part. The paramagnon Boltzmann equation is divided similarly. After this division, the resulting Boltzmann equations have simple interpretations. The equation for the symmetric part of the distribution function describes the balance between the transverse heat flow and the flow of energy out of the paramagnon subsystem into the symmetric part of the electron distribution. The equation for the remaining part describes a balance between the flow of energy from the electron subsystem into the paramagnon subsystem and the Joule heating rate. In order to obtain useful results from these equations, we will go to a limit where the paramagnon distribution is assumed to be thermalized at some temperature $T_{\text{eff}}(E)$. The final step in our analysis will be to show that corrections to the thermal distribution of paramagnons do not change the way in which the current response scales with field.

1. Expanding the Boltzmann equation

The electron distribution function is divided into its symmetric part f^0 (assumed to be a Fermi distribution at a low base temperature that varies slowly across the sample) and the remainder δf. With this notation and after expanding to linear order in δf, the Boltzmann equations may be written in the form

$$\boldsymbol{v}_{\boldsymbol{q}}\cdot\nabla f_{\boldsymbol{q}}^0 = [\mathbf{I}_{\boldsymbol{q}}^{em}(f^0,n)]^S, \tag{23}$$

$$\boldsymbol{E}\cdot\partial_q(f_{\boldsymbol{q}}^0+\delta f_{\boldsymbol{q}}) = [\mathbf{I}_{\boldsymbol{q}}^{em}(f^0,n)]^A + \frac{\delta\mathbf{I}_{\boldsymbol{q}}^{em}}{\delta f_{\boldsymbol{k}}}\delta f_{\boldsymbol{k}}, \tag{24}$$

$$0 = \mathbf{I}_{\boldsymbol{k},\epsilon}^{me}[f^0,n] + \frac{\delta\mathbf{I}_{\boldsymbol{k},\epsilon}^{me}}{\delta f_{\boldsymbol{q}}}\delta f_{\boldsymbol{q}} + \mathbf{I}_{\boldsymbol{k},\epsilon}^{mm}[n]. \tag{25}$$

We have adopted an Einstein convention where terms like $(\delta\mathbf{I}_{\boldsymbol{q}}^{em}/\delta f_{\boldsymbol{k}})\delta f_{\boldsymbol{k}}$ are implicitly integrated over $\boldsymbol{k}$. The superscripts S and A refer to symmetric and nonsymmetric parts of the scattering integrals in $\boldsymbol{q}$. We have allowed for a transverse gradient in f^0 which supports a transverse heat flow.

One might question how, given the fact that we are interested in the nonlinear response, we can use a linear analysis in δf. In a linear response, relaxation-time approximation, the Fermi surface is effectively shifted a distance $\tau_{\text{tr}}eE/\hbar$ in momentum space. Provided this is much less than the Fermi wave vector $(\tau_{\text{tr}}eE/\hbar \ll k_F)$ a linear-response analysis may be applied. In the present case, it turns out that the transport relaxation time, τ_{tr}, self-consistently becomes a power of E so that the resultant current is nonlinear in E.

2. Heat flows

The physical content of Eqs. (23)–(25) is most readily appreciated by considering the energy transfers that they represent. In the case of Eqs. (23) and (24) we multiply by the electron energy $\epsilon_{\boldsymbol{q}}$ and integrate over $\boldsymbol{q}$. In the case of Eq. (25), we multiply by the paramagnon energy ϵ and the spectral density $\rho(\boldsymbol{k},\epsilon)$ and integrate over $\boldsymbol{k}$ and ϵ. After doing this, Eqs. (23)–(25) reduce to

$$0 = \int \frac{d\boldsymbol{q}}{(2\pi)^3}\epsilon_q\{\boldsymbol{v}_{\boldsymbol{q}}\cdot\nabla f_{\boldsymbol{q}}^0 - [\mathbf{I}_{\boldsymbol{q}}^{em}(f^0,n)]^S\}, \tag{26}$$

$$0=\int\frac{d\boldsymbol{q}}{(2\pi)^3}\epsilon_q\left\{\boldsymbol{E}\cdot\partial_q(f_{\boldsymbol{q}}^0+\delta f_{\boldsymbol{q}}) - [\mathbf{I}_{\boldsymbol{q}}^{em}(f^0,n)]^A - \frac{\delta\mathbf{I}_{\boldsymbol{q}}^{em}}{\delta f_{\boldsymbol{k}}}[f^0,n]\delta f_{\boldsymbol{k}}\right\}, \tag{27}$$

$$0 = \int \frac{d\boldsymbol{k}}{(2\pi)^3}d\epsilon\rho(\epsilon,\boldsymbol{k})\epsilon\left[\mathbf{I}_{\boldsymbol{k},\epsilon}^{me}[f^0,n] + \frac{\delta\mathbf{I}_{\boldsymbol{k},\epsilon}^{me}}{\delta f_{\boldsymbol{q}}}[f^0,n]\delta f_{\boldsymbol{q}} + \mathbf{I}_{\boldsymbol{k},\epsilon}^{mm}[n]\right]. \tag{28}$$

Equation (26) may be interpreted as a balance between the transverse heat flow—described by the first term on the right-hand side—and the energy flowing into the symmetrical part of the electron distribution—described by the second term on the right-hand side. The flow of heat into the heat sink has been treated as a boundary condition in writing down this equation. Solving this equation leads to the explicit limit on the sample width discussed in Sec. I and worked out in detail in Ref. 19. We will not concentrate upon it further here.

Equation (27) can be interpreted as a balance between Joule heating—described by the first term on the right-hand side—and the rate at which energy flows from the nonsymmetrical part of the electron distribution into the paramagnon subsystem—described by the second and third terms. To see this requires a little manipulation. The first term may be written explicitly as Joule heating after integrating by parts with respect to $\boldsymbol{q}$.

Equation (28) corresponds to a balance between the rate at which energy flows into the paramagnon subsystem from the symmetrical and nonsymmetrical parts of the electron distribution—described by the first and second terms, respectively. The net flow of energy into the paramagnon subsystem from the electron subsystem is zero in a steady state if we neglect heat flow directly from the paramagnon subsystem to the heat sink. The latter process is ignored since it is much slower than paramagnon-electron scattering. The third term is identically zero, since paramagnon-paramagnon scattering conserves energy. This fact is extremely useful. By considering this integrated equation, one can avoid having to deal explicitly with the paramagnon-paramagnon scattering integral.

We can transform this final equation into a more useful form by using the fact that electron-paramagnon scattering is energy conserving. This implies that

$$\int \frac{d\boldsymbol{q}}{(2\pi)^3}\epsilon_{\boldsymbol{q}}\mathbf{I}^{em}_{\boldsymbol{q}}[f^0,n] = \int \frac{d\boldsymbol{k}}{(2\pi)^3}d\epsilon\epsilon\rho(\epsilon,\boldsymbol{k})\mathbf{I}^{me}_{\boldsymbol{k},\epsilon}[f^0,n],$$

$$\int \frac{d\boldsymbol{q}}{(2\pi)^3}\epsilon_{\boldsymbol{q}}\frac{\delta\mathbf{I}^{em}_{\boldsymbol{q}}}{\delta f_{\boldsymbol{k}}}[f^0,n]\delta f_{\boldsymbol{k}} = \int \frac{d\boldsymbol{k}}{(2\pi)^3}d\epsilon\epsilon\rho(\epsilon,\boldsymbol{k})\frac{\delta\mathbf{I}^{me}_{\boldsymbol{k},\epsilon}}{\delta f_{\boldsymbol{q}}}[f^0,n]\delta f_{\boldsymbol{q}},$$

i.e., the energy entering the electron subsystem from the paramagnon subsystem is equal to the energy entering the paramagnon subsystem from the electron subsystem. Using these results reduces Eq. (28) to the form

$$0 = \int \frac{d\boldsymbol{q}}{(2\pi)^3}\epsilon_{\boldsymbol{q}}\left[\mathbf{I}^{em}_{\boldsymbol{q}}[f^0,n] + \frac{\delta\mathbf{I}^{em}_{\boldsymbol{q}}}{\delta f_{\boldsymbol{k}}}[f^0,n]\delta f_{\boldsymbol{k}}\right]. \tag{29}$$

To make further progress, we must solve the Boltzmann equations explicitly. We will do this to leading order through an approximation that the paramagnon distribution is thermal. We will then argue that corrections to this do not alter the scaling.

3. Thermal paramagnon approximation

Our leading approximation is to assume a thermal distribution of paramagnons, $n_{\boldsymbol{k}}(\epsilon)=n^0(\epsilon)=(e^{\epsilon/T_{\rm eff}}-1)^{-1}$, where the effective temperature is to be determined shortly. In this case, the linearized Boltzmann equations [Eqs. (23)–(25)] reduce to

$$\boldsymbol{v}_{\boldsymbol{q}}\cdot\nabla f^0_{\boldsymbol{q}} = \mathbf{I}^{em}_{\boldsymbol{q}}[f^0,n^0], \tag{30}$$

$$\boldsymbol{E}\cdot\partial_q(f^0_{\boldsymbol{q}}+\delta f_{\boldsymbol{q}}) = \frac{\delta\mathbf{I}^{em}_{\boldsymbol{q}}}{\delta f_{\boldsymbol{k}}}[f^0,n^0]\delta f_{\boldsymbol{k}}, \tag{31}$$

$$0 = \mathbf{I}^{me}_{\boldsymbol{k},\epsilon}[f^0,n^0] + \frac{\delta\mathbf{I}^{me}_{\boldsymbol{k},\epsilon}}{\delta f_{\boldsymbol{q}}}[f^0,n^0]\delta f_{\boldsymbol{q}}. \tag{32}$$

We have used the fact that the paramagnon-paramagnon scattering is identically zero for a thermal distribution of paramagnons. The second equation may be formally solved for δf to obtain

$$\delta f_{\boldsymbol{q}} = \left[1-\left(\frac{\delta\mathbf{I}^{em}}{\delta f}\right)^{-1}\boldsymbol{E}\cdot\partial_q\right]^{-1}\left(\frac{\delta\mathbf{I}^{em}}{\delta f}\right)^{-1}\boldsymbol{E}\cdot\partial_{\boldsymbol{q}}f^0, \tag{33}$$

where we have suppressed momentum labels and integrals over momentum for brevity. Expressions such as $(\delta\mathbf{I}^{em}/\delta f)^{-1}$ are to be understood as matrix inverses with appropriate integrations over momentum in their products. In order to determine the effective temperature, we substitute this solution for δf into the energy-integrated form of Eq. (28) and (31) given by Eq. (29) and expand to leading order in $\boldsymbol{E}$. The result of this substitution is

$$0 = \int \frac{d\boldsymbol{q}}{(2\pi)^3}\epsilon_{\boldsymbol{q}}\left\{\mathbf{I}^{em}_{\boldsymbol{q}} + \boldsymbol{E}\cdot\partial_q\left[\left(\frac{\delta\mathbf{I}^{em}}{\delta f}\right)^{-1}\boldsymbol{E}\cdot\partial_q\delta f\right]\right\}. \tag{34}$$

Integrating the second term by parts reduces it to the form

$$0 = \int \frac{d\boldsymbol{q}}{(2\pi)^3}\epsilon_{\boldsymbol{q}}\left[\mathbf{I}^{em}_{\boldsymbol{q}} - \frac{1}{3}E^2\boldsymbol{v}_{\boldsymbol{q}}\cdot\left(\frac{\delta\mathbf{I}^{em}}{\delta f}\right)^{-1}\partial_q\delta f\right]. \tag{35}$$

The second term is now explicitly the leading-order contribution to the Joule heating rate. This is balanced against the first term which describes the decay of energy from a thermal distribution of paramagnons at temperature $T_{\rm eff}(E)$. Since both the electron and paramagnon distributions involved in the expressions are thermal distributions—at $T=0$ and $T=T_{\rm eff}(E)$, respectively—we may evaluate Eq. (35) using the results of Sec. III. Writing Eq. (35) in terms of the scattering matrices of Sec. III, it can be reduced to

$$\begin{aligned}\int \frac{d\boldsymbol{q}}{(2\pi)^3}\epsilon_{\boldsymbol{q}}\gamma_{\boldsymbol{q}}[1-\mathbf{M}]_{\boldsymbol{qp}}f_{\boldsymbol{p}}(T_0)[1-f_{\boldsymbol{p}}(T_0)] \\ = \int \frac{d\boldsymbol{q}}{(2\pi)^3}\epsilon_{\boldsymbol{q}}\gamma_{\boldsymbol{q}}[1-\mathbf{M}]_{\boldsymbol{qp}}\delta f_{\boldsymbol{p}}.\end{aligned} \tag{36}$$

Substituting for δf to leading order in $\boldsymbol{E}$ from Eq. (31) into Eq. (36), we obtain

$$\begin{aligned}\underbrace{\int \frac{d\boldsymbol{q}}{(2\pi)^3}\epsilon_{\boldsymbol{q}}\cdot\partial_q\{[1-\mathbf{M}]^{-1}_{\boldsymbol{qp}}\gamma^{-1}_{\boldsymbol{p}}\boldsymbol{E}\cdot\partial_{\boldsymbol{q}}f_{\boldsymbol{q}}(T_0)\}}_{\text{Joule heating}} \\ = \underbrace{\int \frac{d\boldsymbol{q}}{(2\pi)^3}\epsilon_{\boldsymbol{q}}\gamma_{\boldsymbol{q}}[1-\mathbf{M}]_{\boldsymbol{qp}}f_{\boldsymbol{p}}(T_0)[1-f_{\boldsymbol{p}}(T_0)]}_{\text{Energy decay from } T_{\rm eff} \text{ to } T_0}.\end{aligned} \tag{37}$$

This equation may be written in the form $d\mathcal{E}/dt \propto E^2\tau_{\rm tr}$ as before in Eq. (3). Since the paramagnon distribution is thermal at temperature $T_{\rm eff}$, using the temperature scaling of the various relaxation rates given in Eq. (17), we find

$$T_{\mathrm{eff}} \propto E^{z/(d+2z-2)}$$

in the high field/temperature limit and d dimensions, implying a nonlinear current

$$j \propto E^{(z-1)/(d+2z-2)}$$

as suggested in Sec. I.

4. Corrections to thermal paramagnon approximation

Corrections to a thermal distribution of paramagnons may be rather large, since in the absence of the electric field the paramagnons are essentially in a zero-temperature distribution. We argue, nevertheless, that corrections to the thermal distribution of paramagnons considered above do not change the scaling of current response. The analysis is similar to the calculation of phonon drag in thermal equilibrium (which similarly does not change the scaling with temperature).

We expand the paramagnon distribution to linear order about the effective thermal distribution; $n=n^0+\delta n$. Substituting into the Boltzmann equations [Eqs. (23)–(25)], we obtain

$$\boldsymbol{v}_{\boldsymbol{q}} \cdot \nabla f^0_{\boldsymbol{q}} = \mathbf{I}^{em}_{\boldsymbol{q}}[f^0,n^0] + \frac{\delta \mathbf{I}^{em}_{\boldsymbol{q}}}{\delta n_{\boldsymbol{k},\epsilon}}[f^0,n^0]\,\delta n^S_{\boldsymbol{k},\epsilon}, \tag{38}$$

$$\boldsymbol{E} \cdot \partial_{\boldsymbol{q}}(f^0_{\boldsymbol{q}} + \delta f_{\boldsymbol{q}}) = \frac{\delta \mathbf{I}^{em}_{\boldsymbol{q}}}{\delta f_{\boldsymbol{k}}}[f^0,n^0]\,\delta f_{\boldsymbol{k}} + \frac{\delta \mathbf{I}^{em}_{\boldsymbol{q}}}{\delta n_{\boldsymbol{k},\epsilon}}[f^0,n^0]\,\delta n^A_{\boldsymbol{k},\epsilon}, \tag{39}$$

$$0 = \mathbf{I}^{me}_{\boldsymbol{k},\epsilon}[f^0,n^0] + \frac{\delta \mathbf{I}^{me}_{\boldsymbol{k},\epsilon}}{\delta f_{\boldsymbol{q}}}[f^0,n^0]\,\delta f_{\boldsymbol{q}} \tag{40}$$

$$+ \frac{\delta \mathbf{I}^{me}_{\boldsymbol{k},\epsilon}}{\delta n_{\boldsymbol{q},\xi}}[f^0,n^0]\,\delta n^S_{\boldsymbol{q},\xi} + \frac{\delta \mathbf{I}^{mm}_{\boldsymbol{k},\epsilon}}{\delta n_{\boldsymbol{q},\xi}}[n^0]\,\delta n_{\boldsymbol{q},\xi}. \tag{41}$$

In Eqs. (38) and (39), δn has been divided into symmetric and nonsymmetric parts δn^S and δn^A. These contribute to the equations for the symmetric and nonsymmetric parts of the electron distribution, respectively. Equation (41) can be solved formally for δn with the result

$$\delta n = \underbrace{-\left(\frac{\delta \mathbf{I}^{me}}{\delta n} + \frac{\delta \mathbf{I}^{mm}}{\delta n}\right)^{-1} \mathbf{I}^{me}}_{\delta n^S} \tag{42}$$

$$\underbrace{-\left(\frac{\delta \mathbf{I}^{me}}{\delta n} + \frac{\delta \mathbf{I}^{mm}}{\delta n}\right)^{-1} \frac{\delta \mathbf{I}^{me}}{\delta f}\,\delta f.}_{\delta n^A} \tag{43}$$

We have identified the spherically symmetric and nonsymmetric parts of δn. Substituting this back into Eqs. (38) and (39) one obtains

$$\boldsymbol{v}_{\boldsymbol{q}} \cdot \nabla f^0_{\boldsymbol{q}} = \mathbf{I}^{em}_{\boldsymbol{q}}[f^0,n^0] - \frac{\delta \mathbf{I}^{em}_{\boldsymbol{q}}}{\delta n}\left(\frac{\delta \mathbf{I}^{me}}{\delta n} + \frac{\delta \mathbf{I}^{mm}}{\delta n}\right)^{-1} \mathbf{I}^{me}, \tag{44}$$

$$\boldsymbol{E} \cdot \partial_{\boldsymbol{q}}(f^0_{\boldsymbol{q}} + \delta f_{\boldsymbol{q}}) = \frac{\delta \mathbf{I}^{em}_{\boldsymbol{q}}}{\delta f_{\boldsymbol{k}}}\,[f^0,n^0]\,\,\delta f_{\boldsymbol{k}} \underbrace{- \frac{\delta \mathbf{I}^{em}_{\boldsymbol{q}}}{\delta n_{\boldsymbol{k},\epsilon}}\left(\frac{\delta \mathbf{I}^{me}}{\delta n} + \frac{\delta \mathbf{I}^{mm}}{\delta n}\right)^{-1} \frac{\delta \mathbf{I}^{me}}{\delta f}\,\delta f.}_{\frac{\delta \mathbf{I}^{eme}}{\delta f}} \tag{45}$$

In the second of these equations, we have adopted the notation of Lifshitz and Pitaevskii[20] identifying this as a term describing a paramagnon-mediated electron-electron interaction. The argument that paramagnon drag does not affect scaling is completed by showing that $\delta \mathbf{I}^{eme}/\delta f$ scales with at least as high a power of T as $\delta \mathbf{I}^{em}/\delta f$. This requires us to go beyond the generic form of the scattering integrals to use their explicit expressions for paramagnon-electron scattering given in the Boltzmann equations [Eqs. (18) and (22)]. Ignoring the paramagnon-paramagnon scattering (it is higher order in T—and hence E—than the paramagnon-electron scattering) we may write

$$\frac{\delta \mathbf{I}^{eme}}{\delta f} = -\frac{\delta \mathbf{I}^{em}_{\boldsymbol{q}}}{\delta n_{\boldsymbol{k},\epsilon}}\left(\frac{\delta \mathbf{I}^{me}}{\delta n} + \frac{\delta \mathbf{I}^{mm}}{\delta n}\right)^{-1} \frac{\delta \mathbf{I}^{me}}{\delta f}. \tag{46}$$

Taking the explicit form of the scattering integrals, the various functional derivatives may be written as

$$\frac{\delta \mathbf{I}^{em}_{\boldsymbol{q}}}{\delta n_{\boldsymbol{k},\epsilon}} = -|g|^2 \rho(\boldsymbol{k},\epsilon)[(f_{\boldsymbol{q}} - f_{\boldsymbol{k}-\boldsymbol{q}})\,\delta(\epsilon - \epsilon_{\boldsymbol{q}} + \epsilon_{\boldsymbol{k}-\boldsymbol{q}}) + (f_{\boldsymbol{q}} - f_{\boldsymbol{k}+\boldsymbol{q}})\,\delta(\epsilon - \epsilon_{\boldsymbol{q}+\boldsymbol{k}} + \epsilon_{\boldsymbol{q}})],$$

$$\frac{\delta \mathbf{I}^{me}_{\boldsymbol{k},\epsilon}}{\delta n_{\boldsymbol{l},\nu}} = |g|^2 \delta(\boldsymbol{l} - \boldsymbol{k})\,\delta(\nu - \epsilon)\int \frac{d\boldsymbol{p}}{(2\pi)^3}(f_{\boldsymbol{p}+\boldsymbol{k}} - f_{\boldsymbol{p}})\,\delta(\epsilon + \epsilon_{\boldsymbol{p}} - \epsilon_{\boldsymbol{p}+\boldsymbol{k}}),$$

$$\frac{\delta \mathbf{I}^{me}_{\boldsymbol{k},\epsilon}}{\delta f_{\boldsymbol{l}}} = |g|^2[-(n_{\boldsymbol{k},\epsilon} + f_{\boldsymbol{l}+\boldsymbol{k}})\,\delta(\epsilon + \epsilon_{\boldsymbol{l}} - \epsilon_{\boldsymbol{l}+\boldsymbol{k}}) + (1 + n_{\boldsymbol{k},\epsilon} - f_{\boldsymbol{l}-\boldsymbol{k}})\,\delta(\epsilon + \epsilon_{\boldsymbol{l}-\boldsymbol{k}} - \epsilon_{\boldsymbol{l}})].$$

Substituting these equations back into Eq. (46) shows that the corrections due to paramagnon drag lead to contributions to the electron-scattering integral that are at least of the same order in temperature as the direct contribution.

IV. CONCLUSIONS AND PROSPECTS

We have considered nonlinear transport near to an itinerant-electron quantum critical point. Since the dynamics near to a quantum critical point are universal and since steady-state out-of-equilibrium distributions are determined by dynamics, we have argued that the universality present near to an equilibrium quantum critical point may be reflected in the out-of-equilibrium behavior.

There are two ways in which a quantum critical itinerant-electron system may be driven out of equilibrium by an electric field. At the highest fields, the rate of Joule heating overwhelms the rate at which heat may be transported out of the system by thermal conduction and the system heats up until the two balance. This mechanism leads to nonlinear response

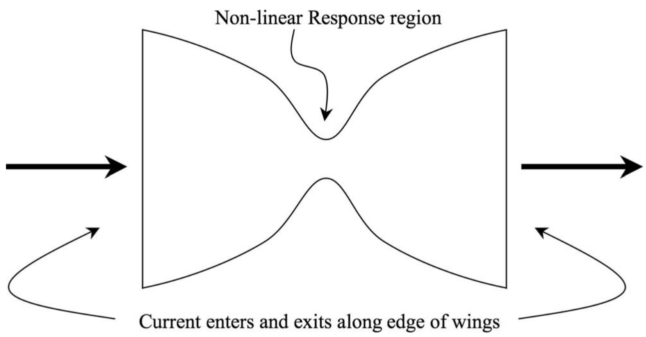

FIG. 1. Schematic diagram of proposed experimental system: (i) Current enters and leaves the bow tie shaped sample along the edges of the wings, reducing contact heating. (ii) Enhanced field and current density in the constriction leads to nonlinear response in this regime. (iii) The extended wings act as a low-temperature heat sink.

in truly bulk samples. We have considered nonlinear response in a restricted geometry where we anticipate that conductivity becomes nonlinear at a lower field governed by the rate at which energy can scatter between the electron and paramagnon subsystems. The resulting conductivity is expected to be independent of sample size and geometry (provided that certain constraints are satisfied). At the lowest fields, the response will return to the linear thermal-equilibrium response.

The existence of the intermediate range of nonlinearity requires restrictions upon the sample width so that thermal conduction can be maintained at a sufficient rate to transport away heat generated by Joule heating. The sample width must nevertheless be sufficient that the paramagnons demonstrate their bulk behavior—i.e., it must be larger than the paramagnon correlation length. Because of the rather different scaling of transport and thermal relaxation lengths with temperature (and hence field), there is a large window of fields within which the type of nonlinearity that we investigate should exist.

What are the prospects for seeing these effects experimentally? We have described a particular experimental geometry in which the heat current is transverse to the electrical current. This enabled the algebra to be readily negotiated. In order to see these effects experimentally, we suggest a slightly different geometry.[21] One possibility is the following: take a bow tie shaped sample with current injected and removed along opposite wings of the bow tie. A current sent through this sample should demonstrate a nonlinear steady state of the type that we have described. The constriction at the center of the bow tie will have enhanced field and current densities and will operate in a nonlinear regime. The injection of current along the extended edge of the bow tie will reduce contact heating; performing the experiment in a pulsed manner will further mitigate these effects. The large heat capacity of the wings of the bow tie compared to the constriction will allow a relatively long pulse time before heat effects become significant; the wings will effectively act as a low-temperature heat sink. A sketch of this arrangement is shown in Fig. 1.

It remains to estimate what field strengths and sample sizes are necessary in order to observe the nonlinear effects that we anticipate. Referring to the analysis at the beginning of the paper, the minimum electric field and maximum sample width are given by

$$E = \frac{k_B T}{e l_{\mathrm{tr}}}, \quad W = \sqrt{l_{\mathrm{tr}} l_{\mathrm{th}}} \sim l_{\mathrm{tr}} (T/\epsilon_F)^{1/z},$$

where the dynamical exponent $z=3$ near to a ferromagnetic critical point. These are strongly temperature dependent, $l_{\mathrm{tr}} \propto T^{-5/3}$, leading to $E \propto T^{8/3}$ and $W \propto T^{-4/3}$ in a three-dimensional quantum critical ferromagnet. For a typical quantum-critical itinerant ferromagnet (e.g., $Sr_3Ru_2O_7$, which has $n=2\times 10^{27}$ m^{-3}, $\sigma=10^9$ Ω^{-1} m^{-1} at 1 K) we estimate[22] that $l_{\mathrm{tr}} \approx 8$ μm and hence $E \approx 10$ Vm^{-1} and $W \approx 400$ nm at 1 K. While these field gradients are achievable, the sample width is too small. Lowering the temperature to 100 mK we estimate $l_{\mathrm{tr}} \approx 400$ μm, $E \approx 2\times 10^{-2}$ V m^{-1}, and $W \approx 9$ μm. This is achievable by standard sample preparation techniques of polishing and etching.[21]

Ultimately, then, the ability to see nonlinear effects in a given quantum critical system is determined by length scale rather than field strength. One must be able to approach close enough to the quantum critical point that the relevant length scales—which would in principle diverge at the quantum critical point—have reached a manageable size. These length scales depend strongly upon temperature and dramatic improvements in potential observability of nonlinear effects may be achieved by lowering the temperature. In many instances, however, new phases are found to appear as the temperature is lowered toward the quantum critical point. Often, this will be the limiting factor: the observability or otherwise of nonlinear effects being determined by whether the length scales have increased sufficiently before the new phase intervenes.

In conclusion, the universal power-law scaling of conductivity near to an itinerant magnetic quantum critical point is reflected in a universal power-law scaling with electric field in the nonlinear conductivity regime. This provides a new way to investigate the consistency between theoretically predicted power laws and those seen experimentally.

ACKNOWLEDGMENTS

This work was supported by the Royal Society and the EPSRC under Grant No. EP/D036194/1. This work was motivated by early conversations with C. Pepin during a visit to Saclay. We would also like to thank S. A. Grigera, C. A. Hooley, and A. P. Mackenzie for comments on the paper.

APPENDIX

In this appendix, we outline the evaluation of the scattering rates given in Eq. (16). The details of the calculation are somewhat similar to that of the same relaxation rate due to phonon scattering. Because of this similarity, our analysis follows quite closely —and makes explicit reference to—the calculation of electron-phonon relaxation rates presented in Chapter 8 of the textbook of Mahan.[23] We shall carry out the calculations in d dimensions, where $d=2$ or 3 in the physical system.

Our first task is to make a few manipulations of the energy relaxation rate to put it in a simplified form. The first step involves using the detailed balance relation expressed in the form

$$\gamma_{pq} = \gamma_{qp}\frac{f_q^T(1-f_p^T)}{f_p^T(1-f_q^T)} = \gamma_{qp}\frac{n^T(\Delta\epsilon_q)}{n^T(\Delta\epsilon_q)+1},$$

where $n^T(\Delta\epsilon_q)$ is the Bose distribution at temperature T and $\Delta\epsilon_q = \epsilon_q - \epsilon_p$. The next step is to integrate over $|\boldsymbol{q}|$ assuming that the $|\boldsymbol{q}|$ dependence of terms other than the Fermi-distribution functions is small and also that the density of electronic states is constant at the Fermi surface. In so doing, we encounter two integrals,

$$I_1(\omega) = \int d\epsilon f(\epsilon)[1-f(\epsilon-\omega)] = \omega n(\omega),$$

$$I_2(\omega) = \int d\epsilon f(\epsilon-\omega)[1-f(\epsilon)] = \omega[n^0(\omega)+1].$$

After these manipulations, the energy relaxation may be expressed as

$$\frac{d\mathcal{E}}{dt} = \frac{1}{2}\int\frac{d^d\boldsymbol{p}\,d^d\hat{\boldsymbol{q}}}{(2\pi)^{2d}}\rho_F\frac{\gamma_{qp}\Delta\epsilon_q^2}{n^T(\Delta\epsilon_q)+1}[n^0(\Delta\epsilon_q)-n^T(\Delta\epsilon_q)],$$

where ρ_F is the electronic density of states at the Fermi surface and the remaining integral over $\boldsymbol{q}$ is just angular; functions of $\boldsymbol{q}$ are to be interpreted as having $|\boldsymbol{q}|$ equal to the Fermi wave vector. The superscripts 0 and T on the Bose-distribution function indicate that they are at the base temperature or the elevated temperature, T, respectively. Notice that this is automatically zero when $T^0 = T$.

In the limit $T^0 \to 0$, we may neglect $n^0(\Delta\epsilon_q)$. Also, in the limit where $\Delta\epsilon_q \ll T$, we may write the energy relaxation in the same form as the other relaxation rates using $n^T(\Delta\epsilon_q)/(n^T(\Delta\epsilon_q)+1) \simeq (1-f_p^T)/(1-f_q^T)$. As all the terms in our scattering rates are now at the elevated temperature T, we will from now on omit this superscript for clarity.

So far, we have reduced our scattering rates to the forms

$$\frac{1}{\tau_q} = \gamma_q = \int\frac{d^d\boldsymbol{p}}{(2\pi)^d}\gamma_{qp}\frac{1-f_p}{1-f_q},$$

$$\frac{1}{\tau_q^{\mathrm{tr}}} = \gamma_q^{\mathrm{tr}} = \int\frac{d^d\boldsymbol{p}}{(2\pi)^d}\gamma_{qp}\frac{1-f_p}{1-f_q}\left[1-\frac{\boldsymbol{q}\cdot\boldsymbol{p}}{q^2}\frac{\gamma_q^{\mathrm{tr}}}{\gamma_p^{\mathrm{tr}}}\right],$$

$$\frac{d\mathcal{E}}{dt} = -\frac{1}{2}\int\frac{d^d\boldsymbol{p}}{(2\pi)^d}\frac{d^d\hat{\boldsymbol{q}}}{(2\pi)^d}\rho_F\Delta\epsilon_q^2\gamma_{qp}\frac{1-f_p}{1-f_q}. \qquad \text{(A1)}$$

In the present case, we are interested in scattering from critical paramagnons. γ_{pq} then takes the form given by Eq. (8). In order to calculate the various relaxation rates explicitly, it is useful to introduce a generalization of the McMillan function. In the discussion of electron-phonon scattering, this takes the form[23]

$$\alpha^2F(E,\omega) = \frac{\hbar}{2\pi}\int\frac{d^d\boldsymbol{q}}{(2\pi)^d}|g_q|^2\delta(\omega-\omega_q)\delta(E-\epsilon_{k+q}), \qquad \text{(A2)}$$

where ω_q is the frequency of a phonon with momentum $\boldsymbol{q}$ and ϵ_p is the energy of an electron with momentum $\boldsymbol{p}$. The generalization of this to scattering from overdamped modes is given by

$$\alpha^2F(E,\omega) = \frac{\hbar}{2\pi}\int\frac{d^d\boldsymbol{q}}{(2\pi)^d}|g_q|^2\rho(\boldsymbol{q},\omega)\delta(E-\epsilon_{k+q}), \qquad \text{(A3)}$$

where $\rho(\boldsymbol{q},\omega) = \mathcal{I}mD^R(\boldsymbol{q},\omega)$ is the paramagnon spectral function. The analogous McMillan function for transport is given by

$$\alpha_t^2F(E,\omega) = -\frac{\hbar}{2\pi}\int\frac{d^d\boldsymbol{q}}{(2\pi)^d}|g_q|^2\frac{\boldsymbol{q}\cdot\boldsymbol{k}}{\boldsymbol{k}^2}\rho(\boldsymbol{q},\omega)\delta(E-\epsilon_{k+q}). \qquad \text{(A4)}$$

The additional angular factors weigh scattering at different angles in the usual way. Equations (A3) and (A4) are the generalizations of Eqs. (8.145) and (8.146) of Ref. 23.

With this identification, expressions for the various scattering integrals may be obtained in the limit $\Delta\epsilon_q \ll T$ as follows [see, for example, Sec. 8.3.1 of Ref. 23—we use $(1-f_p)/(1-f_q) \approx n(\Delta\epsilon_q)$]:

$$\frac{1}{\tau_k} = 2\frac{2\pi}{\hbar}\int_0^\infty d\omega\, n(\omega)\alpha^2F(\epsilon_k,\omega)$$
$$= 2\int_0^\infty d\omega\frac{d^d\boldsymbol{q}}{(2\pi)^d}|g_q|^2 n(\omega)\rho(\boldsymbol{q},\omega)\delta(\epsilon_{k+q}-\epsilon_k), \qquad \text{(A5)}$$

$$\frac{1}{\tau_k^{\mathrm{tr}}} = 2\frac{2\pi}{\hbar}\int_0^\infty d\omega\, n(\omega)\alpha_t^2F(\epsilon_k,\omega)$$
$$= -2\int_0^\infty d\omega\frac{d^d\boldsymbol{q}}{(2\pi)^d}|g_q|^2 n(\omega)\frac{\boldsymbol{q}\cdot\boldsymbol{k}}{\boldsymbol{k}^2}\rho(\boldsymbol{q},\omega)\delta(\epsilon_{k+q}-\epsilon_k), \qquad \text{(A6)}$$

$$\frac{d\mathcal{E}}{dt} = 4\pi\hbar^2\rho_F\int_0^\infty d\omega\, n(\omega)\omega^2\alpha^2F(\epsilon_k,\omega)$$
$$= 2\hbar^3\rho_F\int_0^\infty d\omega\frac{d^d\boldsymbol{q}}{(2\pi)^d}|g_q|^2 n(\omega)\omega^2\rho(\boldsymbol{q},\omega)\delta(\epsilon_{k+q}-\epsilon_k). \qquad \text{(A7)}$$

These integrals may be simplified by first linearizing the electron energy near to the Fermi surface: $\epsilon_{k+q} - \epsilon_k \approx \boldsymbol{v}_k\cdot\boldsymbol{q} = v_F\cos\theta|\boldsymbol{q}|$, where $\boldsymbol{v}_k$ is the Fermi velocity and θ is the angle between $\boldsymbol{k}$ and $\boldsymbol{q}$. Assuming that the matrix element does not have a significant angular dependence—an assumption that is only true for ferromagnets; antiferromagnets have hot lines of scattering on the Fermi surface where electron states are related by the ordering wave vector that lead to complications in this latter case[24]—the angular integrals over $\boldsymbol{q}$ may then be carried out. One then obtains

$$\frac{1}{\tau_{\boldsymbol{k}}} = \frac{2g^2}{(2\pi)^2 v_F}\int_0^\infty d\omega n(\omega)\int^{T/v_F} d|\boldsymbol{q}||\boldsymbol{q}|^{d-2}\rho(\boldsymbol{q},\omega),$$

$$\frac{1}{\tau_{\boldsymbol{k}}^{\mathrm{tr}}} = \frac{2g^2}{(2\pi)^2 v_F}\frac{1}{2k_F^2}\int_0^\infty d\omega n(\omega)\int^{T/v_F} d|\boldsymbol{q}||\boldsymbol{q}|^{d}\rho(\boldsymbol{q},\omega),$$

$$\frac{d\mathcal{E}}{dt} = \hbar^3\rho_F\frac{2g^2}{(2\pi)^2 v_F}\int_0^\infty d\omega n(\omega)\omega^2\int^{T/v_F} d|\boldsymbol{q}||\boldsymbol{q}|^{d-2}\rho(\boldsymbol{q},\omega). \tag{A8}$$

The momentum integral has acquired an explicit cutoff at T/v_F after linearizing the electron energy at the Fermi surface. The remaining integrals may be calculated after explicit substitution of the paramagnon spectral function.

We will evaluate these expressions in both high- and low-temperature limits. Which of these limits one is in is determined by a comparison of $r(T)$ with the typical value of $|\boldsymbol{q}|^2$. The former varies with temperature according to $r(T) \sim T^{(d+z-2)/z}$ and the latter as T^2. In the low-temperature limit $r \gg \boldsymbol{q}^2$ and in the high-temperature limit $r \ll \boldsymbol{q}^2$. In both cases, we consider temperatures much less than the Fermi energy, $T \ll \epsilon_F$.

Carrying out the integrals in the *low-temperature* limit, we find

$$\begin{aligned}\frac{1}{\tau_{\boldsymbol{k}}} &= \frac{2g^2}{(2\pi)^2 v_F}\int_0^\infty d\omega n(\omega)\int_0^{T/v_F} d|\boldsymbol{q}||\boldsymbol{q}|^{d-2}\rho(\boldsymbol{q},\omega)\\ &\sim \int_0^{T/v_F} d|\boldsymbol{q}||\boldsymbol{q}|^{d-2}\int_0^\infty d\omega n(\omega)\frac{\omega/\Gamma_{\boldsymbol{q}}}{r^2+(\omega/\Gamma_{\boldsymbol{q}})^2}\\ &\sim \int_0^{T/v_F} d|\boldsymbol{q}||\boldsymbol{q}|^{d-2}\Gamma_{\boldsymbol{q}}\int_0^\infty \frac{d\omega}{r\Gamma_{\boldsymbol{q}}}n(\omega)\frac{\omega/\Gamma_{\boldsymbol{q}}}{1+(\omega/r\Gamma_{\boldsymbol{q}})^2}\\ &\sim \int_0^{T/v_F} d|\boldsymbol{q}||\boldsymbol{q}|^{d-2}\Gamma_{\boldsymbol{q}}\int_0^\infty du n(ur\Gamma_{\boldsymbol{q}})\frac{u}{1+u^2}\\ &\sim \frac{T}{r(T)}\int_0^{T/v_F} d|\boldsymbol{q}||\boldsymbol{q}|^{d-2}\int_0^\infty du\frac{1}{1+u^2}\\ &\sim \frac{T^d}{r(T)},\end{aligned}$$

where we have used the fact that $r \gg \boldsymbol{q}^2$ at low temperatures. The frequency integral is dominated by the region where ω is up to order $r(T)\Gamma_{\boldsymbol{q}}$. For $\boldsymbol{q} \sim T$, at these frequencies $\omega/T \sim \Gamma r(T)T^{z-3} \ll 1$ and the Bose distribution can be approximated by its low-frequency limit $n(x) \sim T/x$. As a final consistency check, we need to make sure that the dominant momentum $\boldsymbol{q}$ is of the order of T as indeed it is.

A similar evaluation of the transport scattering rate yields the result

$$\frac{1}{\tau_{\boldsymbol{k}}^{\mathrm{tr}}} \sim \frac{T^{d+2}}{r(T)}. \tag{A9}$$

The energy relaxation is given by

$$\begin{aligned}\frac{d\mathcal{E}}{dt} &= \hbar^3\rho_F\frac{2g^2}{(2\pi)^2 v_F}\int_0^\infty d\omega\omega^2 n(\omega)\int_0^{T/v_F} d|\boldsymbol{q}||\boldsymbol{q}|^{d-2}\rho(\boldsymbol{q},\omega)\\ &\sim \int_0^{T/v_F} d|\boldsymbol{q}||\boldsymbol{q}|^{d-2}\int_0^\infty d\omega\omega^2 n(\omega)\frac{\omega/\Gamma_{\boldsymbol{q}}}{r^2+(\omega/\Gamma_{\boldsymbol{q}})^2}\\ &\sim rT\int_0^{T/v_F} d|\boldsymbol{q}||\boldsymbol{q}|^{d-2}\Gamma_{\boldsymbol{q}}^2\int_0^{T/r\Gamma_{\boldsymbol{q}}} du\frac{u^2}{1+u^2}\\ &\sim rT\int_0^{T/v_F} d|\boldsymbol{q}||\boldsymbol{q}|^{d-2}\Gamma_{\boldsymbol{q}}^2\left[\frac{T}{r\Gamma_{\boldsymbol{q}}}-\frac{\pi}{2}\right]\\ &\sim T^2\int_0^{T/v_F} d|\boldsymbol{q}||\boldsymbol{q}|^{d-2}\Gamma_{\boldsymbol{q}}\\ &\sim T^2\int_0^{T/v_F} d|\boldsymbol{q}||\boldsymbol{q}|^{d+z-4}\\ &\sim T^{d+z-1}.\end{aligned} \tag{A10}$$

Carrying out the same integrations in the *high-temperature* limit, we find

$$\begin{aligned}\frac{1}{\tau_{\boldsymbol{k}}} &= \frac{2g^2}{(2\pi)^2 v_F}\int_0^\infty d\omega n(\omega)\int_0^{T/v_F} d|\boldsymbol{q}||\boldsymbol{q}|^{d-2}\rho(\boldsymbol{q},\omega)\\ &\sim \int_0^\infty d\omega n(\omega)\int_0^{T/v_F} d|\boldsymbol{q}||\boldsymbol{q}|^{d-2}\frac{\omega/\Gamma|\boldsymbol{q}|^{z-2}}{q^4+(\omega/\Gamma|\boldsymbol{q}|^{z-2})^2}\\ &\sim \int_0^\infty d\omega n(\omega)\int_0^{T/v_F} d|\boldsymbol{q}||\boldsymbol{q}|^{d+z-4}\frac{\omega}{\Gamma^2\boldsymbol{q}^{2z}+\omega^2}\\ &\sim \int_0^\infty d\omega\frac{n(\omega)}{\omega}\int_0^{T/v_F} d|\boldsymbol{q}|\frac{|\boldsymbol{q}|^{d+z-4}}{\Gamma^2\boldsymbol{q}^{2z}/\omega^2+1}\\ &\sim \int_0^\infty d\omega n(\omega)\omega^{(d-3)/z}\int_0^{(T/v_F)(\Gamma/\omega)^{1/z}} du\frac{u^{d+z-4}}{u^{2z}+1}\\ &\sim T^{(d+z-3)/z}\int_0^\infty dv n(vT)v^{(d-3)/z}\int_0^\infty du\frac{u^{d+z-4}}{u^{2z}+1}\\ &\sim T^{(d+z-3)/z}.\end{aligned} \tag{A11}$$

In carrying out these manipulations we have used the fact that $\frac{T}{v_F}(\frac{\Gamma}{\omega})^{1/z} \to \infty$ at high temperatures, which is consistent since the dominant contribution to the frequency integral comes from $\omega \sim T$. We have rescaled the momentum and frequency integrals and then used the explicit substitution $\Gamma_{\boldsymbol{q}} = \Gamma |\boldsymbol{q}|^{z-2}$. A similar evaluation of the transport scattering rate yields

$$\frac{1}{\tau_{\boldsymbol{k}}^{\mathrm{tr}}} \sim T^{(d+z-1)/z}, \tag{A12}$$

i.e., it carries an extra factor of $\boldsymbol{q}^2 \sim T^{2/z}$ compared to the scattering rate. Finally, the energy relaxation rate is given by

$$\begin{aligned}
\frac{d\mathcal{E}}{dt} &= \hbar^3 \rho_F \frac{2g^2}{(2\pi)^2 v_F} \int_0^\infty d\omega n(\omega)\omega^2 \int_0^{T/v_F} d|\boldsymbol{q}||\boldsymbol{q}|^{d-2} \rho(\boldsymbol{q},\omega) \\
&\sim \int_0^\infty d\omega n(\omega)\omega^2 \int_0^{T/v_F} d|\boldsymbol{q}||\boldsymbol{q}|^{d+z-4} \frac{\omega}{\Gamma^2 \boldsymbol{q}^{2z} + \omega^2} \\
&\sim \int_0^\infty d\omega n(\omega)\omega \int_0^{T/v_F} d|\boldsymbol{q}| \frac{|\boldsymbol{q}|^{d+z-4}}{\Gamma^2 \boldsymbol{q}^{2z}/\omega^2 + 1} \\
&\sim \int_0^\infty d\omega n(\omega)\omega^{(d+2z-3)/z} \int_0^{(T/v_F)(\Gamma/\omega)^{1/z}} du \frac{u^{d+z-4}}{u^{2z}+1} \\
&\sim T^{(d+3z-3)/z} \int_0^\infty dv n(vT) v^{(d+2z-3)/z} \int_0^\infty du \frac{u^{d+z-4}}{u^{2z}+1} \\
&\sim T^{(d+3z-3)/z}.
\end{aligned} \tag{A13}$$

[1] S. Sachdev, *Quantum Phase Transitions* (Cambridge University Press, Cambridge, England, 1999).

[2] S. L. Sondhi, S. M. Girvin, J. P. Carini, and D. Shahar, Rev. Mod. Phys. **69**, 315 (1997).

[3] P. Coleman and A. J. Schofield, Nature (London) **433**, 226 (2005).

[4] T. Moriya, *Spin Fluctuations in Itinerant Electron Magnetism* (Springer-Verlag, Berlin, 1985).

[5] J. A. Hertz, Phys. Rev. B **14**, 1165 (1976).

[6] A. J. Millis, Phys. Rev. B **48**, 7183 (1993).

[7] D. Dalidovich and P. Phillips, Phys. Rev. Lett. **93**, 027004 (2004).

[8] A. G. Green and S. L. Sondhi, Phys. Rev. Lett. **95**, 267001 (2005).

[9] A. G. Green, J. E. Moore, S. L. Sondhi, and A. Vishwanath, Phys. Rev. Lett. **97**, 227003 (2006).

[10] K. Damle and S. Sachdev, Phys. Rev. B **56**, 8714 (1997).

[11] M.-C. Cha, M. P. A. Fisher, S. M. Girvin, M. Wallin, and A. P. Young, Phys. Rev. B **44**, 6883 (1991).

[12] Nonlinear response near to quantum criticality has also been discussed by J. Fenton and A. J. Schofield, Phys. Rev. Lett. **95**, 247201 (2005), although in their case, the system remains in thermal equilibrium.

[13] T. Oka and H. Aoki, Phys. Rev. Lett. **95**, 137601 (2005).

[14] A. Mitra, S. Takei, Y. B. Kim, and A. J. Millis, Phys. Rev. Lett. **97**, 236808 (2006).

[15] In a previous work considered by one of us (Ref. 8), the situation was rather simpler since the thermal conductivity of the model system considered was formally infinite and therefore there was no limit to the rate at which Joule heat could be transported.

[16] The relation that the present work bears to Ref. 14 is rather similar to the relation that Ref. 7 bears to Ref. 8.

[17] J. Rech, C. Pépin, and A. V. Chubukov, Phys. Rev. B **74**, 195126 (2006).

[18] The expression for the transport relaxation rate is arrived at by first substituting the form $\delta f_{\boldsymbol{p}} = g(|\boldsymbol{p}|)\boldsymbol{p}\cdot\boldsymbol{E}$ into the scattering integral,

$$\begin{aligned}
\gamma_{\boldsymbol{q}}[1-M]_{\boldsymbol{qp}}\delta f_{\boldsymbol{p}} &= \int \frac{d\boldsymbol{p}}{(2\pi)^3}\left[\gamma_{\boldsymbol{qp}} \frac{1-f_{\boldsymbol{p}}}{1-f_{\boldsymbol{q}}} g(|\boldsymbol{q}|)\boldsymbol{q}\cdot\boldsymbol{E} \right. \\
&\quad \left. - \gamma_{\boldsymbol{pq}} \frac{1-f_{\boldsymbol{q}}}{1-f_{\boldsymbol{p}}} g(|\boldsymbol{p}|)\boldsymbol{p}\cdot\boldsymbol{E}\right] \\
&= \int \frac{d\boldsymbol{p}}{(2\pi)^3} \gamma_{\boldsymbol{qp}} \frac{1-f_{\boldsymbol{p}}}{1-f_{\boldsymbol{q}}}\left[g(|\boldsymbol{q}|)\boldsymbol{q}\cdot\boldsymbol{E} \right. \\
&\quad \left. - \frac{f_{\boldsymbol{q}}(1-f_{\boldsymbol{q}})}{f_{\boldsymbol{p}}(1-f_{\boldsymbol{p}})} g(|\boldsymbol{p}|)\boldsymbol{p}\cdot\boldsymbol{E}\right] \\
&= \int \frac{d\boldsymbol{p}}{(2\pi)^3} \gamma_{\boldsymbol{qp}} \frac{1-f_{\boldsymbol{p}}}{1-f_{\boldsymbol{q}}}\left[g(|\boldsymbol{q}|)\boldsymbol{q}\cdot\boldsymbol{E} \right. \\
&\quad \left. - \frac{\partial_\epsilon f_{\boldsymbol{q}}}{\partial_\epsilon f_{\boldsymbol{p}}} g(|\boldsymbol{p}|)\boldsymbol{p}\cdot\boldsymbol{E}\right] \\
&= \delta f_{\boldsymbol{q}} \int \frac{d\boldsymbol{p}}{(2\pi)^3} \gamma_{\boldsymbol{qp}} \frac{1-f_{\boldsymbol{p}}}{1-f_{\boldsymbol{q}}}\left[1 - \frac{\partial_\epsilon f_{\boldsymbol{q}}}{\partial_\epsilon f_{\boldsymbol{p}}} \frac{g(|\boldsymbol{q}|)\boldsymbol{q}\cdot\boldsymbol{E}}{g(|\boldsymbol{p}|)\boldsymbol{p}\cdot\boldsymbol{E}}\right].
\end{aligned}$$

The final manipulation to get this to the same form as above to use the fact that within the relaxation-time approximation $g(\boldsymbol{p}) = \partial_\epsilon f_{\boldsymbol{p}} / m\gamma_{\boldsymbol{p}}^{\mathrm{tr}}$.

[19] The heat sink is strictly necessary to permit the formation of a steady state. It will not appear explicitly in our analysis, which will be essentially linear response for the electrons. The actual answer will turn out to be nonlinear in the electric field because of the field dependence of the paramagnon-electron-scattering rate. For an interesting discussion of the role of the heat sink in conductivity measurements see A.-M. Tremblay, B. Patton, P. C. Martin, and P. F. Maldague, Phys. Rev. A **19**, 1721 (1979).

[20] E. M. Lifshitz and L. P. Pitaevskii, *Physical Kinetics*, Course of Theoretical Physics Vol. 10 (Butterworth-Heinemann, Oxford, 1981), Sec. 82.

[21] S. A. Grigera (private communication).

[22] In order to estimate the transport length at 1 K, we have used the Drude formula $\sigma = ne^2\tau/m$ and $n = k_F^3/(3\pi^2)$ to obtain $l_{tr} = (\hbar\sigma/e^2)(3\pi^2/n^2)^{1/3}$. The temperature dependence of the transport length is given by Eq. (17). The Fermi energy of $Sr_3Ru_2O_7$ is $\epsilon_F/k_B = (\hbar^2/2k_B m)(3\pi^2 n)^{2/3} \approx 7\times 10^3$ K.

[23] G. D. Mahan, *Many-Particle Physics* (Kluwer, New York, 2000).

[24] A. Rosch, Phys. Rev. Lett. **82**, 4280 (1999).